ENVIRONMENTAL RESEARCH
LETTERS



OPEN ACCESS

RECEIVED
24 January 2026

REVISED
3 April 2026

ACCEPTED FOR PUBLICATION
24 April 2026

PUBLISHED
27 May 2026



LETTER

# Atlantic multidecadal variability modulates extratropical summer heatwaves

**Kunhui Ye*** **and Tim Woollings**

Atmospheric, Oceanic and Planetary Physics, University of Oxford, Oxford, United Kingdom
* Author to whom any correspondence should be addressed.

**E-mail:** kunhui.ye@physics.ox.ac.uk

**Keywords:** Atlantic multidecadal variability, heatwave, atmospheric circulation, land surface and heat fluxes, linear and nonlinear interactions

Supplementary material for this article is available online

## Abstract

Atlantic multidecadal variability (AMV) is a well-known mode of climate variability with well-understood impacts on several aspects of Northern Hemisphere climate. However, its impact on heatwaves, a type of heat extremes that is increasingly affecting human societies, remains less well understood. The influence of AMV on extratropical summer heatwaves in the Northern Hemisphere is analyzed with a suite of coupled climate model experiments from the Decadal Climate Prediction Project. Our analysis suggests that AMV exerts substantial influence on the heatwave frequency (HWF) and heatwave number (HWN) of heatwaves over subtropics and midlatitudes in the Northern Hemisphere. Compared to the widespread seasonal mean warming response, these heatwave hotspots are less expansive geographically. The warm AMV phase (AMV+) as opposed to the cold phase (AMV−) drives a global stationary wave anomaly that links hotspots of HWF and HWN increases over North America, North Africa, central/western Asia, and parts of East Asia. Such dynamic impacts of AMV on heatwaves are more significant than the thermodynamic impacts of a warmer ocean surface. Hence, mean surface warming alone due to the warming effects of AMV+ versus AMV− does not necessarily equate to more frequent heatwaves. Furthermore, precipitation and surface heat fluxe responses further amplify the HWF increases. By further comparing the tropical and extratropical portions of AMV imposed in model simulations, we emphasize that linear and nonlinear interactions of these features strongly shape the impacts of AMV. We further discuss the mechanisms for and causes of model-observation discrepancies and inter-model uncertainties in the influence of AMV on atmospheric circulation and summer heatwaves, in terms of atmospheric circulation response in North Atlantic-Europe and jet waveguide effects. This highlights some challenges in pinpointing the influence of AMV on heatwaves, and improved understanding of it is necessary for more accurate predictions and projections of heatwaves.

## 1. Introduction

Atlantic multidecadal variability (AMV) is a major mode of multidecadal variations in sea surface temperatures (SSTs) over the North Atlantic [1]. AMV thus is important for climate variability on decadal-multidecadal timescales. While the underlying mechanisms for AMV remain debated [2–8], it has been linked to climate and weather variability within and beyond the North Atlantic-European sector with both thermodynamic and dynamic effects [9–18]. Overall, the impacts of AMV on climate variability are well documented and studied. However, the impacts of AMV on weather extremes such as summer heatwaves are less well understood. Heatwaves have become more frequent and intense in a warming climate [19]. Understanding the multidecadal modulation of these heatwaves by AMV can help to predict and understand their multidecadal variability. Both decadal variability and external forcings will shape temperatures over the coming decades and the former is underestimated by models [20]. A

deeper understanding of how decadal-multidecadal variability affects heatwaves is needed to understand the range of possible heatwave occurrences. The phase transition of AMV has been shown to drive decadal-multidecadal variations of extreme high temperature [21] and heatwaves [22, 23] in the Northern Hemisphere (NH). AMV is linked to many hotspots of extreme high temperature variations in summer via a barotropic circumglobal teleconnection [21]. AMV is also found to modulate the occurrence of heatwaves in the Euro-Mediterranean region [24]. The influence of AMV on European summer heatwaves is limited to regions around the Mediterranean Basin [25]. AMV is found to drive changes in summer heatwave days in North America [26], which is mostly attributed to the tropical North Atlantic SST anomalies. It is not clear whether the tropical SST anomalies of AMV also dominates for other regions in terms of impacting decadal-multidecadal heatwave variations. However, it is challenging to isolate the impacts of AMV using observational analysis owning to limited historical records of AMV, presence of other modes of climate variability and the impacts of external forcings.

The Decadal Climate Prediction Project (DCPP) [27], contributing to the sixth Coupled Model Intercomparison Project, has coordinated a dedicated set of coupled climate simulations to address the impacts of AMV. Coupled model simulations from DCPP suggest that the positive phase of the AMV (AMV+ hereafter) compared to the negative phase of the AMV (AMV−) excites a prominent stationary wave anomaly during wintertime over the extratropics in the NH [28]. This has driven significant climate variability over the NH including precipitation and temperature. These DCPP experiments and similar model experiments have been analyzed for the impact of AMV+ versus AMV− on regional heatwaves [24–26]. In this study, we analyze a set of the latest DCPP large-ensemble coupled model experiments available from two climate models (CNRM-CM6-1 and HadGEM3-GC31-MM) to study the impacts of AMV on five metrics of heatwaves during the extended NH summer (May–September) for the extratropics of the NH. In addition, we explicitly compare the relative contributions of the tropical and extratropical SST anomalies of AMV in driving the changes in heatwaves. We compare the link of heatwaves to AMV phase change between observations and model outputs to discuss agreements and discrepancies, and their implications. Note that our study focuses on the internal component of AMV as outlined in the next section. This paper is organized as follows. Section 2 provides descriptions of the data and DCPP coupled model experiments. Major results are discussed in section 3, which is followed by a Summary and discussion.

## 2. Data and methodology

### 2.1. ERA5, CRU, HadEX3 data and heatwave indices

Geopotential height at 500 hPa (Z500), converted by dividing geopotential by 9.8, and zonal wind at 200 hPa (U200) with a resolution of 0.25° from the fifth generation of atmospheric reanalysis by the European Centre for Medium-Range Weather Forecasts [29] are used. Surface air temperature (SAT) is from the Climatic Research Unit gridded Time Series (**CRU TS v. 4.09**). HadEX3 data from the Met Office Hadley Centre provides five characteristic aspects of heatwaves including heatwave frequency (HWF), heatwave number (HWN), heatwave amplitude (HWA), heatwave duration (HWD) and heatwave magnitude (HWM) for extended summers (May–September for the NH) [30]. These indices are computed following the World Meteorological Organization's Expert Team on Sector-Specific Climate Indices (ET-SCI). Heatwaves are defined as having at least three consecutive days that exceed the 90th percentile thresholds of the daily maximum temperature (TX). The 90th percentile thresholds are computed for each calendar day using a 15-day moving window over the chosen reference period (1981–2010). HWF is the sum of days that contribute to heatwave events in the extended summers. HWN is the number of heatwave events. HWA is the peak daily temperature of the hottest heatwave that has the highest mean temperature. HWD is the length in days of the longest heatwave. HWM is the mean temperature of heatwave events. Therefore, HWN/HWF describes the occurrence of heatwaves while HWM/HWA describes the strength of heatwaves. In this study, we focus on extratropical summer heatwaves (north of 20° N) as the percentile-based heatwave definition is more applicable to extratropical regions [19].

### 2.2. AMV index and DCPP idealized AMV experiments

The component C experiments of DCPP project provide idealized coupled climate simulations by restoring SSTs over the North Atlantic to study the impacts of AMV+/−. For full AMV+/− SST restoring, the region is between 10°–65° N; for tropical or extratropical AMV+/− SST restoring, the region is shown in the paper by Boer *et al* [27]. A buffer zone of 8° outside the boundaries of the region is applied with decreasing restoring strength to smooth the boundaries and minimize shocks. A restoring coefficient of 40 $W\,m^{-2}\,K^{-1}$, equivalent to a time scale of about 2 months for a 50 m deep mixed layer, is used. The AMV index (figure 1(a)) and its associated SST anomaly patterns are shown in Boer *et al* [27]. The AMV SST anomaly patterns correspond to one standard deviation of the AMV

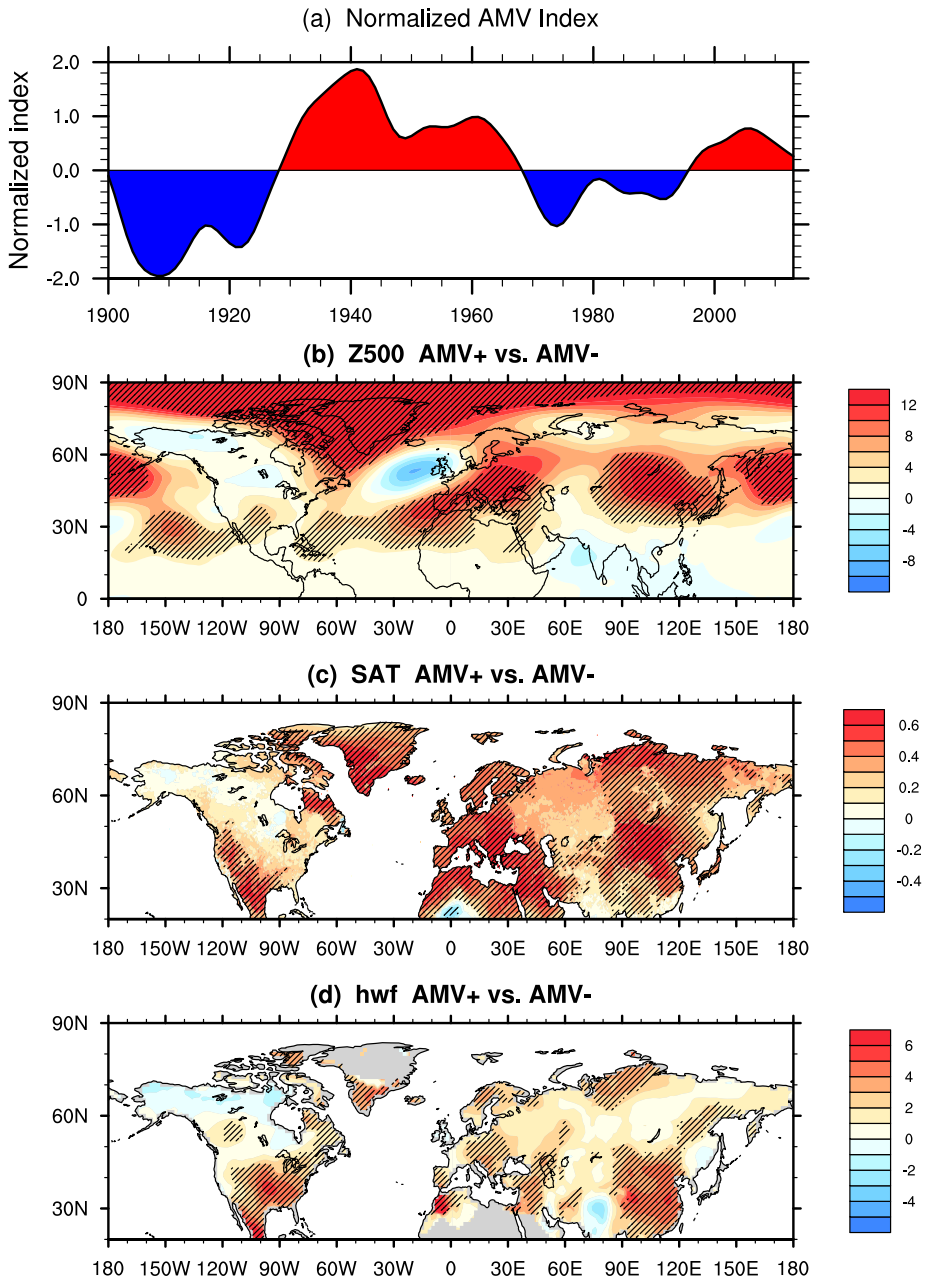


**Figure 1.** (a) Normalized index of Atlantic Multidecadal Variability from 1900 to 2013 from the DCPP project. Composited differences in (b) geopotential height at 500 hPa, (c) surface air temperature, (d) heatwave frequency between warm and cold phases of AMV . Hatching indicates differences significant at the 5% level according to the bootstrap method. Units: gpm for geopotential height, °C for temperature and days for heatwave frequency. Geopotential height is taken from the ERA5 data. Surface air temperature and heatwave frequency are from the Climatic Research Unit gridded Time Series (**CRU TS v. 4.09**) and from HadEX3 data provided by the Met Office Hadley Centre respectively.

index relative to the 12 month model climatology. These SST anomaly patterns are superimposed on the model climatology to minimize drift. Global warming trends are removed when computing the AMV index [3]. Preindustrial control values are prescribed for all the external forcings. To ensure a fair comparison between these experiments and observations/ERA5, linear detrending is applied to observations/ERA5 data for the composite analysis as described in the next subsection. However, the jets and stationary waves are still highly similar between the ERA5 and model control experiment, suggesting that the prescription of preindustrial external forcing may not affect interpretation of the results. We note that active SST-restoring in the tropical North Atlantic may cause unrealistic local SST-surface heat flux relationships and exaggerate the subsequent climatic impacts [31]. However, the conclusion from the study is qualitative and is subject to further discussions. Quantifying such local SST-surface heat flux relationships and obtaining a 'pure' SST pattern forcing are difficult given the coupling nature of air-sea interactions. The use of one standard deviation of anomaly, rather than larger than this, in the

AMV SST pattern may potentially compensate for any exaggeration of the impacts. Nonetheless, these model experiments provide important insights into the impacts of AMV on climate variability. They offer important large-ensemble data for mechanistic understanding that observations are not able to provide.

TX data from two models (CNRM-CM6-1 and HadGEM3-GC31-MM) were available at the time of analysis for identifying heatwaves in the idealized AMV experiments. Seven coupled experiments from the DCPP project are analyzed for the two models. These experiments are dcppC-atl-control, dcppC-amv-pos/neg, dcppC-amv-Trop-pos/neg and dcppC-amv-ExTrop-pos/neg, representing restoring SST towards model control run climatology, restoring SST towards AMV+/−, restoring SST towards tropical AMV+/−, and restoring SST towards extratropical AMV+/−, respectively. These experiments are run for 10 years with 40 ensemble members for CNRM-CM6-1 and 25 ensemble members for HadGEM3-GC31-MM, which differ in oceanic initial conditions [28]. Some variables however have fewer ensemble members due to data availability. The last 9 years are used in the analysis with the first year discarded. More details of the DCPP project can be found in [27, 28]. To compute the five heatwave aspects, we use the Climpact software package, following the ETSCI methodology as in the HadEX3 data. For each ensemble member, the 90th percentile thresholds are computed from the dcppC-atl-control experiments over the last 9 years of simulations before heatwave aspects are determined for other experiments. Daily TX is not available in dcppC-amv-Trop-pos/neg and dcppC-amv-ExTrop-pos/neg experiments for CNRM-CM6-1; results on heatwaves are thus not available for these experiments for CNRM-CM6-1.

### 2.3. Composite analysis and bootstrap method for significance test

For the composite analysis based on the AMV index (figure 1), ERA5 and HadEX3 data are first linearly detrended by removing the least squares linear trend. Warm and cold AMV years are determined from an overlapping period 1940–2013. For the models, all available ensemble members are used in the composite analysis. Statistical significance for all the composite analyses is assessed using the bootstrap method with 1000 resampling times. The bootstrap method randomly selects two groups of samples respectively from AMV+/− years for ERA5/HadEX3 with replacement and then performs the composite analysis. For model experiments, the bootstrap method randomly selects two groups of samples respectively from AMV+/− model experiments with replacement. Composited differences are statistically significant if they fall within the 95% confidence level of the bootstrapped values and the confidence level range does not straddle zero. The bootstrap method does not assume an underlying distribution of the data and offers a reliable way to quantify sampling uncertainty.

### 2.4. Jet stream and stationary wave in dcppC-atl-control model experiment and ERA5

To understand the potential underlying mechanisms for model differences and model-ERA5 discrepancies, we compare the extratropical jets, distribution of zonal wave number (Ks) [32] and stationary wave pattern between Atlantic control experiments from the models and ERA5 (figure S1). Here, we apply unsmoothed longitudionally varying U200 to computing Ks. The results suggest that the jet is weaker in CNRM-CM6-1 (figure S1(d)) than in ERA5 (figure S1(a)) while HadGEM3-GC31-MM (figure S1(g)) shows a comparable one. The discrepancy is particularly noticeable for the Asian jet. The jets are long considered as waveguides for Rossby waves underpinned by large Ks magnitude. Comparing the Ks distributions suggests that CNRM-CM6-1 model has some discontinuity in Ks (without valid Ks) over Europe and Asia along the jet waveguide, largely not seen in both HadGEM3-GC31-MM and ERA5. This potentially leads to a breakdown or weakening in the Asian jet waveguide in CNRM-CM6-1. We further note that the stationary wave pattern computed for Z500 is more consistent between HadGEM3-GC31-MM and ERA5. For example, CNRM-CM6-1 has a weaker negative anomaly over western Canada and North Atlantic, and a positive anomaly stretching too far east. Overall, CNRM-CM6-1 has less realistic jets, waveguide and stationary wave compared to HadGEM3-GC31-MM when using ERA5 as a reference.

## 3. Results

### 3.1. Decadal-multidecadal modulation of summer heatwaves by AMV phase change

AMV exhibited roughly two cycles throughout the period 1900–2013 and was in a warm phase in recent decades (figure 1(a)). A prominent stationary-wave circulation anomaly pattern over mid-high latitudes is seen to accompany AMV+ as opposed to AMV−, with notable high pressure anomaly centers across the midlatitudes (figure 1(b)). The atmospheric circulation anomaly shows a negative summer North Atlantic Oscillation (SNAO). A similar atmospheric circulation pattern is seen for the NCEP-NCAR Reanalysis 1 data [33] (not shown). Widespread warming anomalies are seen in the extratropical regions, particularly over western North America, Greenland, Europe, North Africa, Mideast and East

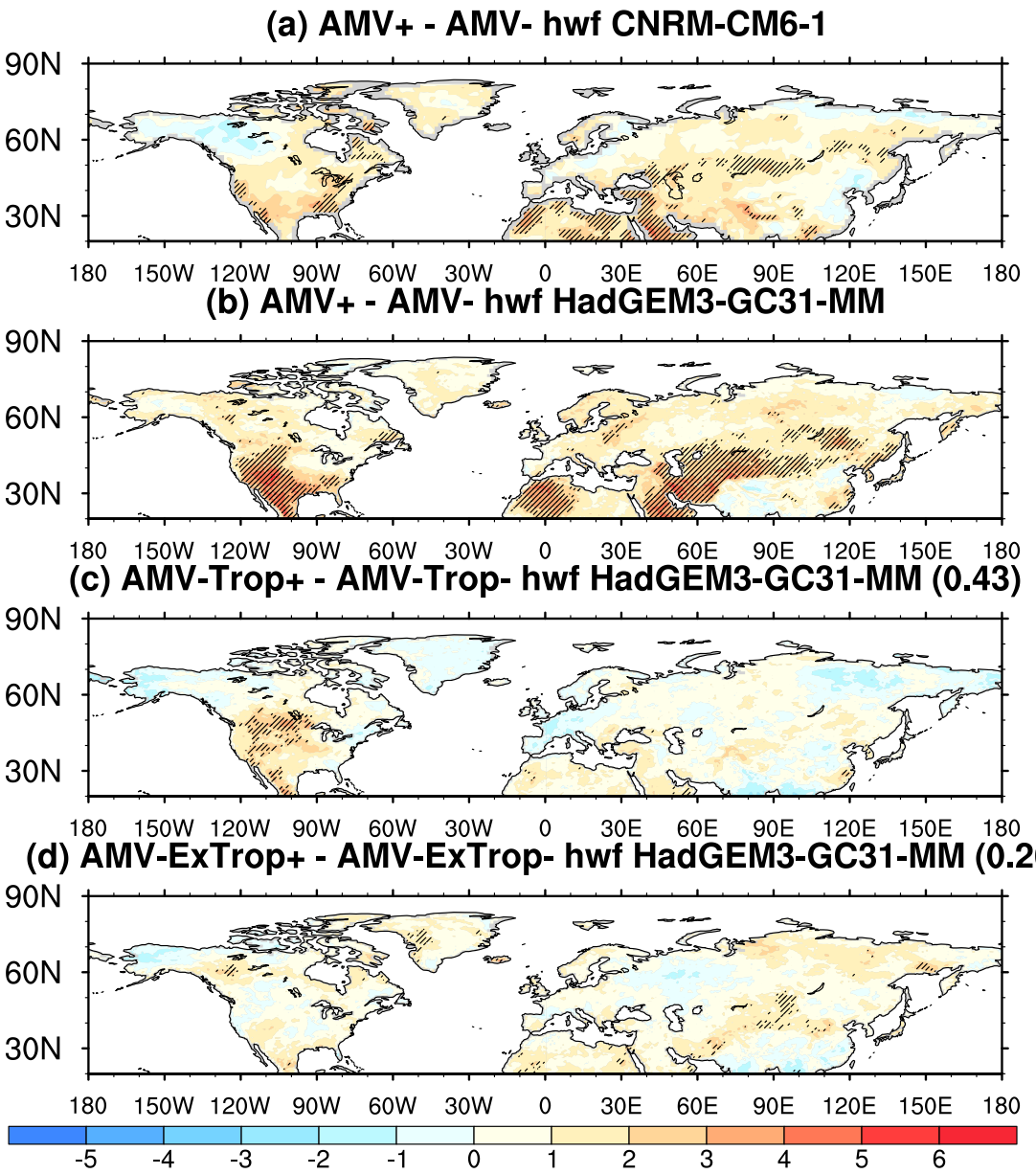


**Figure 2.** Composited differences in heatwave frequency between warm and cold phases of AMV for the DCPP idealized coupled climate model simulations. The meaning of hatching is as in figure 1. Units: days for heatwave frequency. Numbers in the titles of panels (c) and (d) show the spatial correlation between the panels and the full-AMV experiment in panel (b).

Eurasia (figure 1(c)). AMV is linked to summer multidecadal SAT variability over Eurasia via wave-train-like atmospheric circulation [34]. The high-pressure anomalies may enhance the warming by suppressing cloud formation, increasing shortwave radiation and by favoring descent and adiabatic warming [19, 35].

Significant increases in HWF over many regions are observed, but are evidently less widespread compared to SAT (figure 1(d)). The HWN shows similar anomalies to HWF (figure S2(a)) and less so for HWD (figure S2(b)). For both HWM and HWA (figures S2(c) and (d)), the anomalies are mostly not statistically significant. The increases in HWF are mostly dominated by the change in HWN in the subtropics and midlatitudes, for example the European region. Quantitatively, the largest mean HWF increase is as large as 5–6 days per summer, corresponding to an increase of about 1 heatwave event per summer. Comparing figures 1(b)–(d) suggests that the presence of high height anomalies generally explains the distribution of HWF anomalies, while in contrast the mean SAT distribution is not always consistent with HWF anomalies. For example, significant warming in western Europe is paired with weak HWF anomaly accompanied by a cyclonic anomaly to the west of Europe. This suggests a dominant role of dynamic effects over thermodynamic warming linked to the AMV influence.

The DCPP experiments are analyzed to provide modeling evidence for quantifying the influence of AMV on summer heatwaves (figure 2). Significant increases in HWF are seen in both models

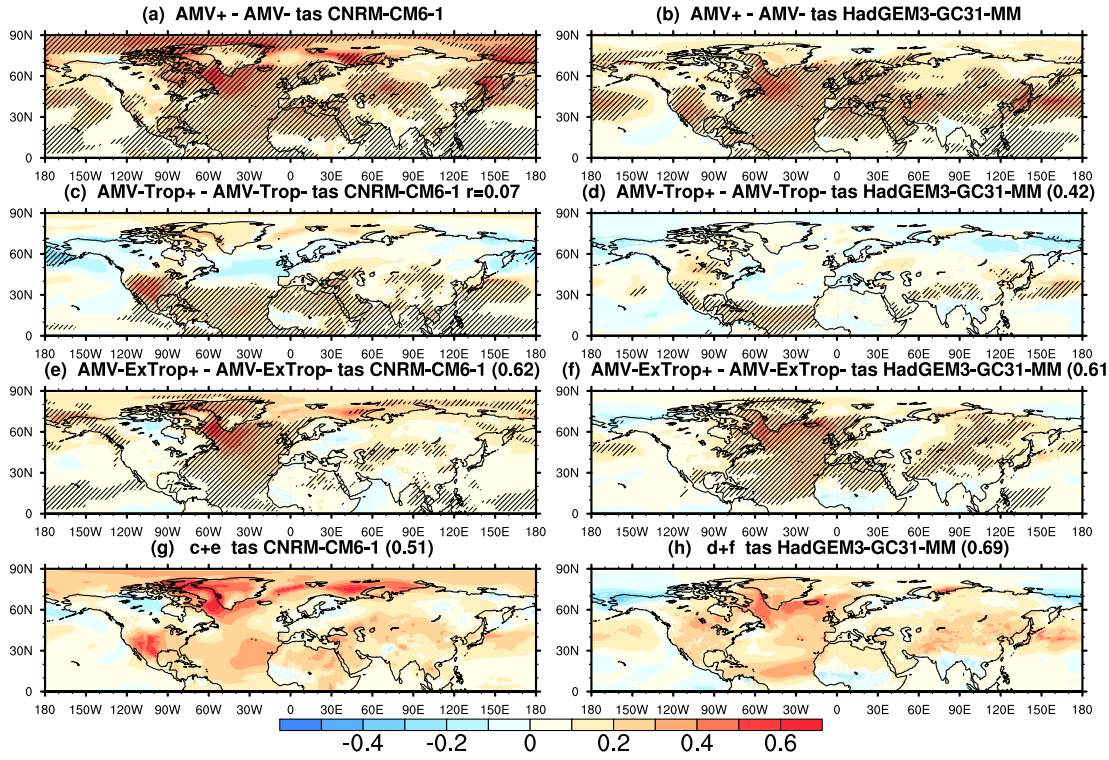


**Figure 3.** Similar to figure 2 but for composited differences in surface air temperature. The meaning of hatching is as in figure 1. Units: °C. Panels (g) and (h) are the sum of panels (c) and (e), and of (d) and (f), respectively.

(figures 2(a) and (b)), mostly south of 50° N and with the HadGEM3-GC31-MM model having stronger responses. The HWN response (figures S3(a) and (b)) is similar to that of HWF, consistent with the observations. The impacts on HWD (figures S3(c) and (d)) are still relatively strong for the HadGEM3-GC31-MM model but are mostly weak on HWM and HWA (figures S3(e)–(h)), consistent with the observations/reanalysis. Thus, AMV+ compared to AMV− increases the number and frequency of summer heatwaves but does not affect much the strength of heatwaves. Comparing models and observations, the common hotspots of significant increases in HWF are North America, North Africa, central/western Asia, and parts of East Asia. In the models, the largest mean HWF increase is about 4–5 days (about 0.8 heatwave events) per summer, similar to observations. On the other hand, significant HWF increases over southern and eastern Europe and China as observed in the HadEX3 data (figure 1(d)) are not seen in the models. These discrepancies are linked to the atmospheric circulation anomalies as discussed below.

As in observations/reanalysis, the modeled SAT response to AMV impacts is more widespread than the HWF (figures 3(a) and (b)). For example, there are virtually no significant HWF increases while there are significant warming anomalies in Europe. Therefore, the mean warming effects of AMV do not necessarily mean increasing HWF. Heatwave events are by definition extremes within seasons, and seasonal-mean warming does not necessarily suggest an increase in their frequency. However, comparing figures 2 and 3 suggests that regions with relatively larger increases in mean SAT tend to have increases in HWF, largely reflecting the extreme temperature impacts on mean temperature. This can be further explained by the Z500 response (figures 4(a) and (b)), which resembles a global stationary wave pattern superimposed on a general increase in height, particularly in the tropics and subtropics. The modeled stationary wave pattern is similar in character to the reanalysis-based Z500 anomaly, albeit with an eastward phase shift for the CNRM-CM6-1 model in particular. This may be related to the underestimated SNAO response in the models, leading to less strong wave source, and weakened waveguide effects over Europe and Central Asia in CNRM-CM6-1 model (see section 2.4).

The model discrepancy is largely explained by their differences in the jets and waveguide in the control experiment (see section 2.4). The model-ERA5 discrepancy is likely related to the circulation response in the North Atlantic-European sector, for example a weaker SNAO response in the models. The modeled Z500 anomaly captures the low height anomaly over Europe and the high height anomaly over the North America, North Africa-eastern Europe and eastern Asia. As in observations/reanalysis, the circulation pattern response strongly shapes the HWF anomaly in response to an AMV phase change. The position and phase of the excited stationary wave

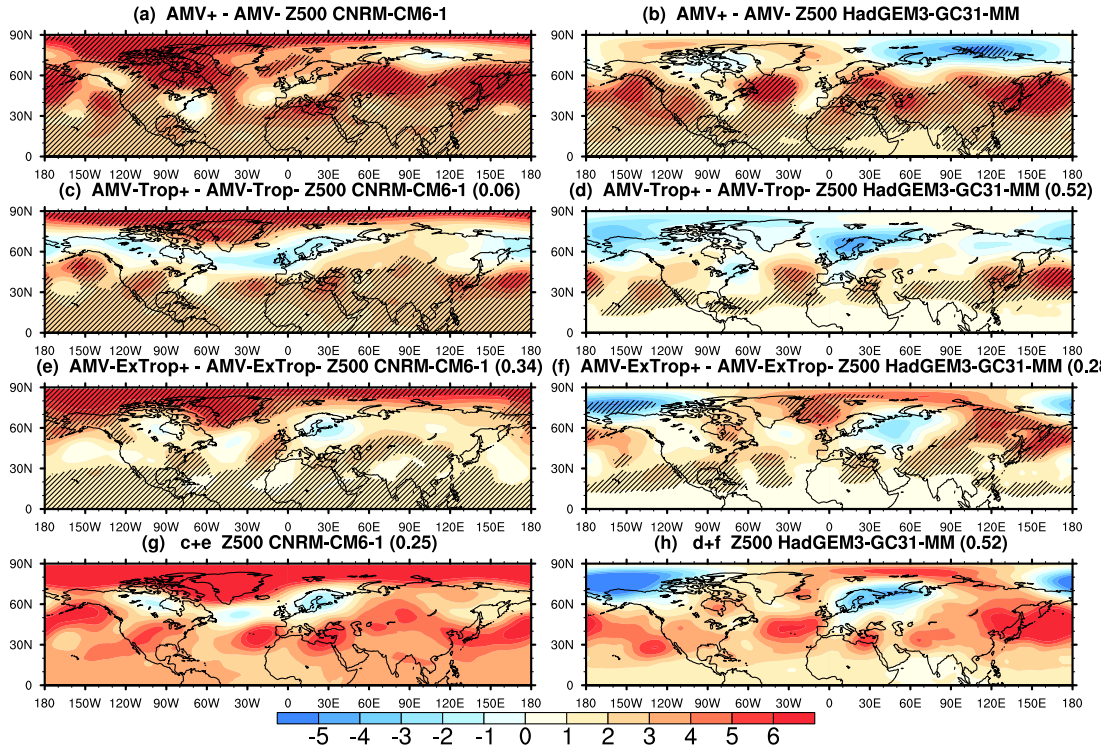


**Figure 4.** As in figure 3 but for geopotential height at 500 hPa. Units: gpm.

pattern plays a significant role in driving changes in HWF in the subtropics and midlatitudes. To further support this, we select those ensembles better capturing the reanalysis-based Z500 circulation patterns (spatial pattern correlation >=0.3) and find stronger heatwave response compared to the response based on all ensembles (figure S4). The spatial pattern of HWF response is also more consistent with observations and the SNAO response is stronger, better resembling that in ERA5 (not shown). This supports the dominant role of atmospheric circulation in linking AMV phase change to heatwaves in the extratropics of the NH. It also suggests that capturing the SNAO-like response is important for capturing the global stationary wave train associated with AMV phase change and the relevant impacts on HWF. In the next subsection, we further demonstrate the role of land surface feedback in inter-model discrepancy in terms of HWF response. Further contributing factors such as internal variability, model uncertainties/biases and background states are discussed in the discussion section.

### 3.2. Precipitation, turbulent and radiation fluxes associated with AMV impacts

Land surface feedbacks in terms of soil moisture and associated heat fluxes have been considered to play an important role in driving heatwaves in North America [19, 26]. Precipitation affects surface radiation to modulate surface energy balance, thus affecting surface temperature and heatwaves. It also affects surface soil moisture, which is an important contributor to heatwaves [25]. In addition, upward sensible heat flux towards the underlying atmosphere also affects heatwaves by affecting surface heat budget. To better understand how AMV drives large-scale changes to modulate heatwaves in the extratropics, the responses of precipitation, turbulent heat fluxes and downward shortwave radiation are given in figure 5. Downward (upward) heat flux is positive (negative). Note that the downward shortwave radiation dominates the net shortwave radiation change. AMV+ increases precipitation over the tropical North Atlantic (figures 5(a) and (b)), driven by a significant increase in turbulent heat fluxes (figures 5(e)–(h)). The enhanced precipitation in the tropical North Atlantic has been linked to high pressure anomalies over western North America [10], leading to an increase in heatwave occurrence in the region [26]. This is related to enhanced tropical Atlantic upward motion by SST warming, potential northward shift of the Intertropical Convergence Zone and a Matsuno–Gill atmospheric response [10, 26]. The high-pressure anomaly in western North America leads to less precipitation, more downward shortwave radiation (figures 5(c) and (d)), less soil moisture (not shown, only available for the CNRM-CM6-1 model), less latent heat flux and more sensible heat flux in the region, further amplifying the heatwave anomaly. This is more pronounced for the HadGEM3-GC31-MM model. These effects are also notable over central Asia and to some extent the regions around the Lake Baikal in the HadGEM3-GC31-MM model. In contrast, more precipitation and less shortwave radiation correspond to

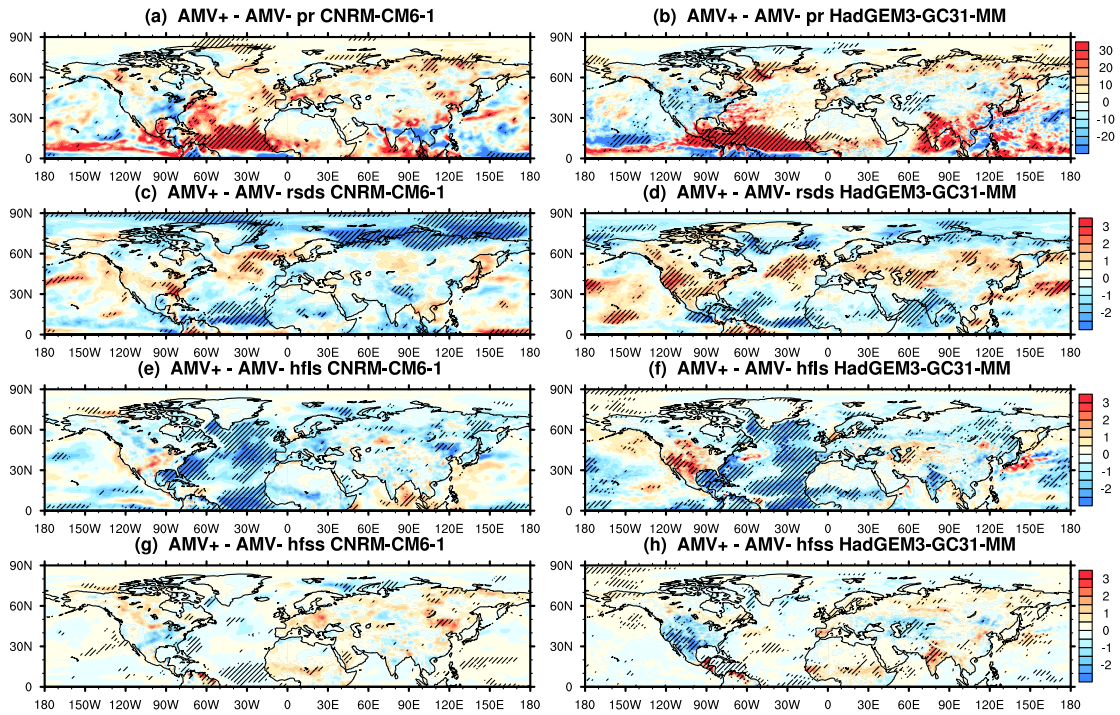


**Figure 5.** As in figure 3 but for (a), (b) precipitation, (c), (d) downward shortwave radiation, (e), (f) surface latent heat flux and (g), (h) surface sensible heat flux. Units: mm for precipitation and W $m^{-2}$ for heat fluxes.

reduced HWF in Europe, offsetting and potentially cancelling the effects of increased mean temperature. This is further modulated by more latent heat flux and less sensible heat flux.

To further understand modulation of AMV on the radiative and turbulent heat fluxes, we compare the monthly area-mean anomalies for Southwest North America, Central Asia and East Eurasia in the two models (figure 6). In both models, the sensible heat flux shows consistently negative anomaly while the latent heat flux shows consistently positive values from May to September in Southwest North America (figures 6(a) and (b)). This is coupled with some reduction in precipitation in both models and, in HadGEM3-GC31-MM, increased net shortwave and reduced net longwave radiation. These changes suggest that AMV drives persistent anomalies in land surface process and downward radiation to impact summer heatwaves. These climatic anomalies favor the occurrence of heatwaves (figures 2(a) and (b)), consistent with the decadal modulation of heatwaves by AMV. A similar situation is seen in Central Asia for HadGEM3-GC31-MM (figure 6(d)), corresponding to large HWF increase. The monthly anomalies are less persistent throughout the season for CNRM-CM6-1 (figure 6(c)). In East Eurasia, less heat flux towards the underlying atmosphere and cooling effect of increasing latent heat flux throughout the season are less conducive to HWF increase in CNRM-CM6-1 (figure 6(e)). No persistent anomalies are seen for other variables. Net shortwave radiation shows a persistent positive anomaly, which may be partly offset by the persistent negative latent heat flux in HadGEM3-GC31-MM (figure 6(f)). The sensible heat flux anomaly is weak throughout the season. Land surface feedbacks may dampen the effects of increasing net shortwave radiation associated with the high pressure anomaly (figures 4(a) and (b)) on heatwaves in East Eurasia. Overall, land surface feedbacks do seem to amplify HWF anomaly in Southwest North America in both models with a larger effect in HadGEM3-GC31-MM, and in Central Asia for HadGEM3-GC31-MM. Therefore, the land surface feedback is also a contributing factor to more significant HWF increase in HadGEM3-GC31-MM than in CNRM-CM6-1.

### 3.3. Contributions of tropical and extratropical portions of AMV

Coupled model experiments with the tropical and extratropical parts of the AMV SST pattern restored separately [27] are analyzed to compare their relative contributions to the heatwave response. While restoring one part of the AMV SST pattern, SST of the other regions is still free to evolve. However, assuming the overlying atmospheric temperature is closely related to SST, this experiment protocol is still reasonable given that SAT anomalies in the other regions are either not significant or weakly warmer for these experiments (figures 3(c)–(f)). Further, analysis of turbulent heat fluxes response suggests passive SST response in the free SST-evolving regions (not shown). In terms of HWF response pattern, the tropical portion of AMV has a larger spatial correlation

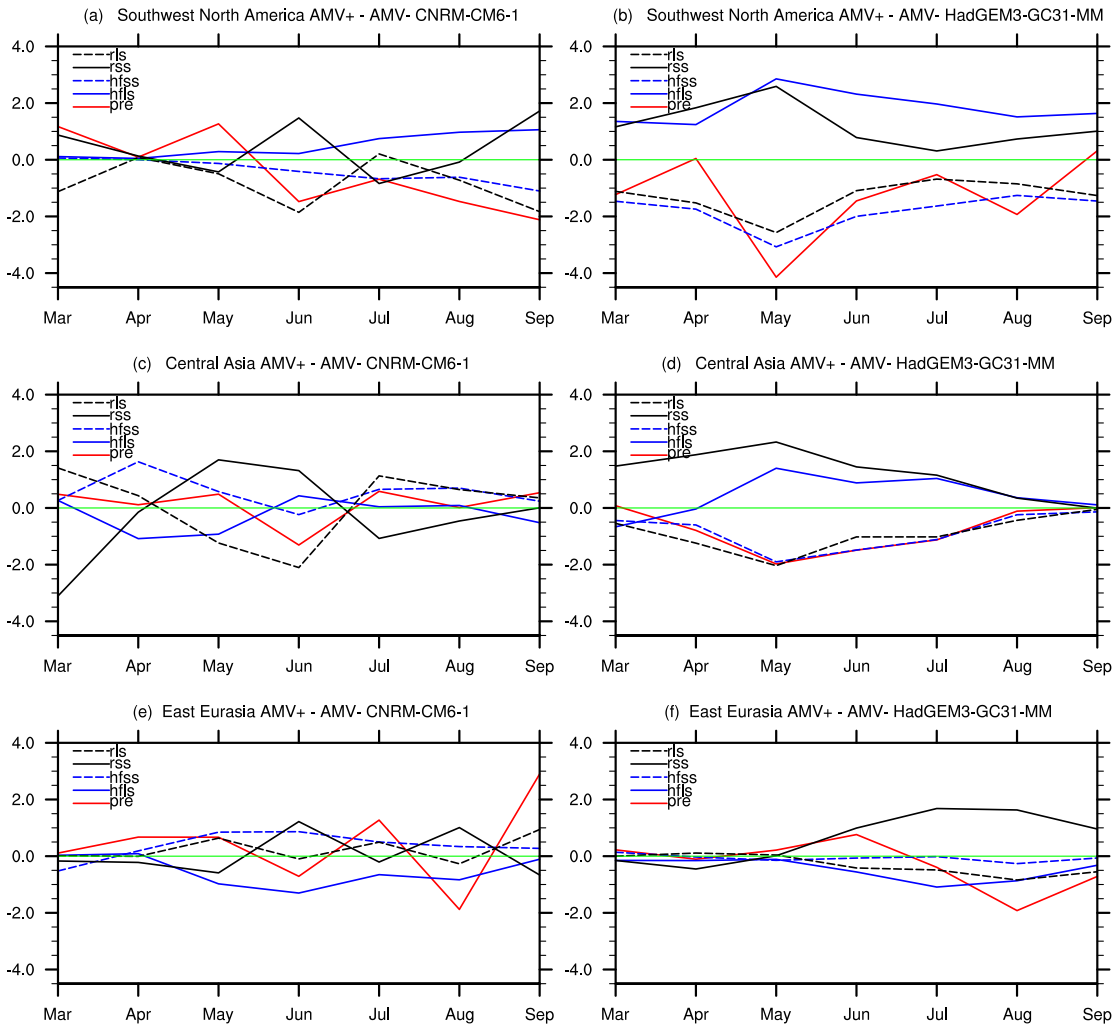


**Figure 6.** Monthly evolutions of the area-mean composited differences for Southwest North America (a), (b), Central Asia (c), (d) and East Eurasia (e), (f) for precipitation (red), surface latent heat flux (solid blue) surface sensible heat flux (dashed blue), net shortwave radiation (solid black) and longwave radiation (dashed black). Reference line of zero is in green. Left (right) panels are for CNRM-CM6-1 (HadGEM3-GC31-MM). Units are mm for precipitation and W $m^{-2}$ for heat fluxes.

of 0.43 than the extratropical portion (0.26) with the full AMV (figures 2(c) and (d)). The former has stronger impacts on HWF in North America while the latter seems to have stronger impacts in the Eurasian region. We define linear interactions as a simple addition of the two experiments with tropical or extratropical AMV SST pattern restored. Nonlinear interactions are inferred by comparing the full-AMV pattern experiment with the addition of these experiments with tropical or extratropical AMV SST pattern restored. The linear addition of tropical and extratropical AMV SST pattern experiments (not shown) gives a spatial correlation of 0.47, explaining less than 25% of the total spatial variance of the HWF anomaly from the full-AMV response. This suggests that the tropical and extratropical portions interact both linearly and nonlinearly to produce the full-AMV impacts.

Such linear and nonlinear interactions are further understood by comparing their respective impacts on SAT and Z500 in figures 3 and 4. Significant surface warming induced by the tropical AMV portion is mostly located in the lower latitudes while that by the extratropical AMV portion obviously extends further north but does also include some tropical warming (figures 3(c)–(f)) [36]. The extratropical AMV portion equally better captures the full-AMV response for both models. However, for the CNRM-CM6-1 model, the tropical AMV portion poorly captures the full-AMV response. Their linear addition gives a higher spatial correlation for HadGEM3-GC31-MM than for CNRM-CM6-1.

Nonlinear interactions between the tropical and extratropical components of AMV are also significant for the Z500 response in particular over the extratropics (see figure 4). The linear addition explains much less of the spatial variance of the full-AMV response for both models, particularly for the CNRM-CM6-1 model. The tropical portion of AMV does not well reproduce the stationary wave structure for the

CNRM-CM6-1 model compared to the HadGEM3-GC31-MM model. This is an important reason why the linearly-added AMV response explains less spatial variance of the full-AMV response in the CNRM-CM6-1 model. In this regard, atmospheric circulation response to tropical SST forcing may be an important source for model uncertainty in the impact of AMV on climate variability and extremes. Without the nonlinear interactions, both the modeled tropical and extratropical portions of AMV have relatively weak contributions to the HWF change (figures 2(e)–(f)).

We note that tropical AMV SST forcing produces more localized SAT response than extratropical AMV SST forcing in both models. As discussed in section 2.4, there are two major waveguides linked to the North Atlantic and Asian jets. A subtropical perturbation in North Africa is found to excite a wave train propagating along the Asian jet waveguide, while that over the midlatitude North Atlantic is seen to excite two wave trains propagating along the Asian jet waveguide and the North Atlantic jet waveguide over Northern Eurasia [32]. This largely explains the Z500 response to tropical and extratropical AMV SST forcing (figures 4(c)–(f)) and the subsequent impacts on SAT. For the extratropical AMV SST forcing, the SAT response is stronger in HadGEM3-GC31-MM than in CNRM-CM6-1. This is related to better jet representation and waveguides in HadGEM3-GC31-MM (see section 2.4 for details). Therefore, we suggest that the teleconnection patterns in HadGEM3-GC31-MM better represent observed AMV teleconnections, consistent with the above discussion.

## 4. Discussions and conclusions

While our analysis focuses on the role of AMV in multidecadal summer heatwaves variability, other drivers are also important for understanding their variability on both interannual and multidecadal timescales. These include cryospheric changes [37] , midlatitude atmospheric blocking [38, 39], the Western Pacific subtropical high [40], land-air coupling [41], El Niño-Southern Oscillation [22], Indian Ocean Dipole [42],and Pacific Decadal Oscillation [43]. Future comprehensive studies addressing the interactions of multiple drivers will clearly be beneficial for understanding summer heatwave variability.

We analyze HadEX3 data, ERA5 reanalysis and seven coupled model experiments from the DCPP project to investigate the impacts of AMV on summer HWF in the extratropics in the NH. Our analysis suggests that AMV+ significantly increases summer heatwaves in terms of frequency and number of events over some hotspot regions in the extratropics compared to AMV−. On the other hand, its influence on heatwave strength characterized by HWM/HWA is minimal. We also identify a global stationary wave anomaly that dominates the heatwave responses compared to the general warming effects of AMV+ versus AMV-. Comparisons of the two models available for analysis indicate that details of the global stationary wave anomaly have significant influences on the magnitude and location of the HWF increase. Apart from these, precipitation, radiative and turbulent heat fluxes also play a role in amplifying the summer heatwave anomalies. We also compare the relative contributions of the tropical and extratropical AMV portions and find that nonlinear interactions between them are important for capturing the full AMV responses. This means that considering the full AMV pattern and its representation in both observational analysis and climate modeling is important to assess the full impacts of AMV.

The modeled responses confirm several hotspots of the summer heatwaves in extratropics as seen in observations/reanalysis in response to AMV phase change. This suggests that decadal-multidecadal variability of summer heatwaves is modulated by AMV phase change. AMV is thus important for future projections of summer heatwaves in the NH as a source of natural variations for heatwave change. However, we note that the modeled responses of summer heatwaves to AMV phase change are generally weaker than those linkages based on observations/reanalysis. For example, the linkages between AMV and summer heatwaves are notable over China in observations/reanalysis but their links are weak and mostly absent in models. We compare the atmospheric circulation anomaly and find that the modeled Z500 global stationary wave anomaly pattern exhibits weaker magnitude and a phase shift compared to the ERA5 reanalysis. The discrepancies in these global stationary wave responses can largely account for the model-observations differences. Differences in the background state, for example due to the use of preindustrial external forcings in model experiments as well as model biases, may be one plausible reason contributing to the discrepancies. Internal variability is another plausible reason for such discrepancies. The two models available for analysis exhibit considerable differences in the circulation and heatwave responses, highlighting model-dependent uncertainties in the impacts of AMV on summer heatwaves.

The inter-model and model-observation/ERA5 discrepancies are largely explained by the models' simulations of the extratropical jets and their waveguide effects. This suggests that further understanding of the large-scale atmospheric circulation representation in models is important for interpreting the responses to AMV forcing. Model uncertainties in the atmospheric circulation response have been noted in previous studies [17, 18, 28]. As the climate state changes, the interaction of regional AMV with global warming could significantly modify the summer stationary waves and heatwave distributions [44, 45], and the amplified warming in the Arctic may

modulate large-scale planetary wave activity [46]. An AMV-like phase change is found to account for a substantial fraction of European heatwave trend during 1980–2021 [39]. Understanding and constraining model differences in the atmospheric circulation response to AMV is important for prediction and projection of summer heatwaves changes in the extratropics of the NH.

## Acknowledgments

KY was supported by the UKRI Horizon Europe Guarantee MSCA Postdoctoral Fellowship EP/Y029119/1, and by the John Fell Fund financed by Oxford University Press (Project Reference: 0013106). We thank the modeling groups that contributed to the DCPP project.

## Data availability statement

NCEP-NCAR Reanalysis 1 data is provided by the NOAA PSL, Boulder, Colorado, USA, from their website at https://psl.noaa.gov.

The data that support the findings of this study are openly available at the following URL/DOI: https://cds.climate.copernicus.eu; www.metoffice.gov.uk/hadobs/hadex3; https://esgf-node.llnl.gov/search/cmip6/; https://crudata.uea.ac.uk/cru/data/hrg/cru_ts_4.09/cruts.2503051245.v4.09/tmp/; https://psl.noaa.gov/data/gridded/data.ncep.reanalysis.html [47].

## Conflict of interest

The author declares no competing interests.

## References

[1] Schlesinger M E and Ramankutty N 1994 An oscillation in the global climate system of period 65–70 years *Nature* **367** 723–6
[2] Latif M, Collins M, Pohlmann H and Keenlyside N 2006 A review of predictability studies of Atlantic sector climate on decadal time scales *J. Clim.* **19** 5971–87
[3] Ting M, Kushnir Y, Seager R and Li C 2009 Forced and internal twentieth-century SST trends in the North Atlantic *J. Clim.* **22** 1469–81
[4] Delworth T L and Mann M E 2000 Observed and simulated multidecadal variability in the Northern Hemisphere *Clim. Dyn.* **16** 661–76
[5] Enfield D B, Mestas-Nuñez A M and Trimble P J 2001 The Atlantic Multidecadal Oscillation and its relation to rainfall and river flows in the continental U.S. *Geophys. Res. Lett.* **28** 2077–80
[6] Clement A, Bellomo K, Murphy L N, Cane M A, Mauritsen T, Rädel G and Stevens B 2015 The Atlantic Multidecadal Oscillation without a role for ocean circulation *Science* **350** 320–4
[7] O'Reilly C H, Huber M, Woollings T and Zanna L 2016 The signature of low-frequency oceanic forcing in the Atlantic Multidecadal Oscillation *Geophys. Res. Lett.* **43** 2810–8
[8] Bellucci A, Mariotti A and Gualdi S 2017 The role of forcings in the twentieth-century North Atlantic multidecadal variability: the 1940–75 North Atlantic cooling case study *J. Clim.* **30** 7317–37
[9] Sutton R T and Hodson D L R 2005 Atlantic ocean forcing of North American and European summer climate *Science* **309** 115–8
[10] Sutton R T and Hodson D L R 2007 Climate response to basin-scale warming and cooling of the North Atlantic ocean *J. Clim.* **20** 891–907
[11] Zhang R and Delworth T L 2006 Impact of Atlantic multidecadal oscillations on India/Sahel rainfall and Atlantic hurricanes *Geophys. Res. Lett.* **33** L17712
[12] Knight J R, Folland C K and Scaife A A 2006 Climate impacts of the Atlantic Multidecadal Oscillation *Geophys. Res. Lett.* **33** L17706
[13] Hodson D L R, Sutton R T, Cassou C, Keenlyside N, Okumura Y and Zhou T 2010 Climate impacts of recent multidecadal changes in Atlantic Ocean Sea Surface Temperature: a multimodel comparison *Clim. Dyn.* **34** 1041–58
[14] Sutton R T and Dong B 2012 Atlantic ocean influence on a shift in European climate in the 1990s *Nat. Geosci.* **5** 788–92
[15] Peings Y and Magnusdottir G 2014 Forcing of the wintertime atmospheric circulation by the multidecadal fluctuations of the North Atlantic ocean *Environ. Res. Lett.* **9** 034018
[16] O'Reilly C H, Woollings T and Zanna L 2017 The dynamical influence of the Atlantic multidecadal oscillation on continental climate *J. Clim.* **30** 7213–30
[17] Ruprich-Robert Y, Msadek R, Castruccio F, Yeager S, Delworth T and Danabasoglu G 2017 Assessing the climate impacts of the observed Atlantic multidecadal variability using the GFDL CM2.1 and NCAR CESM1 global coupled models *J. Clim.* **30** 2785–810
[18] Hodson D L R *et al* 2022 Coupled climate response to Atlantic multidecadal variability in a multi-model multi-resolution ensemble *Clim. Dyn.* **59** 805–36
[19] Domeisen D, Eltahir E, Fischer E, Knutti R, Perkins-Kirkpatrick S, Schär C, Seneviratne S I, Weisheimer A and Wernli H 2023 Prediction and projection of heatwaves *Nat. Rev. Earth Environ.* **4** 36–50
[20] O'Reilly C H, Befort D J, Weisheimer A, Woollings T, Ballinger A and Hegerl G 2021 Projections of northern hemisphere extratropical climate underestimate internal variability and associated uncertainty *Commun. Earth Environ.* **2** 194
[21] Gao M, Yang J, Gong D, Shi P, Han Z and Kim S-J 2019 Footprints of Atlantic multidecadal oscillation in the low-frequency variation of extreme high temperature in the Northern Hemisphere *J. Clim.* **32** 791–802
[22] Zhou Y and Wu Z 2016 Possible impacts of mega-El Niño/Southern Oscillation and Atlantic Multidecadal Oscillation on Eurasian heatwave frequency variability *Q. J. R. Meteorol. Soc.* **142** 1647–61
[23] Lei N, Guan X, Xie Y, Shen X, Ding Y and Huang J 2025 Decadal oceanic variability amplified recent heatwave in the Northern Hemisphere *npj Clim. Atmos. Sci.* **8** 292
[24] Qasmi S, Sanchez-Gomez E, Ruprich-Robert Y, Boé J and Cassou C 2021 Modulation of the occurrence of heatwaves over the euro-mediterranean region by the intensity of the Atlantic multidecadal variability *J. Clim.* **34** 1099–114
[25] Mascolo V, Priol C L, D'Andrea F and Bouchet F 2025 Comparing the influence of Atlantic multidecadal variability and spring soil moisture on European summer heat waves *Oxford Open Clim. Change* **5** 023
[26] Ruprich-Robert Y, Delworth T, Msadek R, Castruccio F, Yeager S and Danabasoglu G 2018 Impacts of the Atlantic

multidecadal variability on North American summer climate and heat waves *J. Clim.* **31** 3679–700
[27] Boer G J *et al* 2016 The Decadal Climate Prediction Project (DCPP) contribution to CMIP6 *Geosci. Model Dev.* **9** 3751–77
[28] Ruggieri P *et al* 2021 Atlantic multidecadal variability and North Atlantic jet: a multimodel view from the decadal climate prediction project *J. Clim.* **34** 347–60
[29] Hersbach H *et al* 2020 The ERA5 global reanalysis *Q. J. R. Meteorol. Soc.* **146** 1999–2049
[30] Dunn R J H *et al* 2024 Observed global changes in sector-relevant climate extremes indices—an extension to HadEX3 *Earth Space Sci.* **11** e2023EA003279
[31] O'Reilly C H, Patterson M, Robson J, Monerie P A, Hodson D and Ruprich-Robert Y 2023 Challenges with interpreting the impact of Atlantic multidecadal variability using SST-restoring experiments *npj Clim. Atmos. Sci.* **6** 14
[32] Hoskins B J and Ambrizzi T 1993 Rossby wave propagation on a realistic longitudinally varying flow *J. Atmos. Sci.* **50** 1661–71
[33] Kalnay E *et al* 1996 The NCEP/NCAR 40-year reanalysis project *Bull. Am. Meteorol. Soc.* **77** 437–70
[34] Hu Y, Zuo Z, Chen H and Hua W 2025 Attribution of multidecadal summer temperature variations over Eurasia *Environ. Res. Lett.* **20** 054005
[35] Röthlisberger M and Papritz L 2023 Quantifying the physical processes leading to atmospheric hot extremes at a global scale *Nat. Geosci.* **16** 210–6
[36] Dunstone N J, Smith D M and Eade R 2011 Multi-year predictability of the tropical Atlantic atmosphere driven by the high latitude North Atlantic ocean *Geophys. Res. Lett* **28** 14701
[37] Ye K, Cohen J, Chen H W, Zhang S, Luo D and Hamouda M E 2025 Attributing climate and weather extremes to Northern Hemisphere sea ice and terrestrial snow: progress, challenges and ways forward *npj Clim. Atmos. Sci.* **8** 166
[38] Li M, Yao Y, Simmonds I, Luo D, Zhong L and Chen X 2020 Collaborative impact of the NAO and atmospheric blocking on European heatwaves, with a focus on the hot summer of 2018 *Environ. Res. Lett.* **15** 114003
[39] Luo B, Luo D, Zhuo W, Xiao C, Dai A, Simmonds I, Yao Y, Diao Y and Gong T 2023 Increased summer European heatwaves in recent decades: contributions from greenhouse gases-induced warming and Atlantic multidecadal oscillation-like variations *Earth's Future* **11** e2023EF003701
[40] Liu Q, Zhou T, Mao H and Fu C 2019 Decadal variations in the relationship between the Western pacific subtropical high and summer heat waves in East China *J. Clim.* **32** 1627–40
[41] Zhang K, Zuo Z, Mei W, Zhang R and Dai A 2025 A westward shift of heatwave hotspots caused by warming-enhanced land–air coupling *Nat. Clim. Change* **15** 546–53
[42] Behera S, Ratnam J V, Masumoto Y and Yamagata T 2013 Origin of extreme summers in Europe: the Indo-Pacific connection *Clim. Dyn.* **41** 663–76
[43] Ren X, Liu W, Capotondi A, Amaya D J and Holbrook N J 2023 The Pacific Decadal Oscillation modulated marine heatwaves in the Northeast Pacific during past decades *Commun. Earth Environ.* **4** 218
[44] Shaw T and Voigt A 2015 Tug of war on summertime circulation between radiative forcing and sea surface warming *Nat. Geosci.* **8** 560–6
[45] Baker H S, Woollings T, Mbengue C, Allen M R, O'Reilly C H, Shiogama H and Sparrow S 2019 Forced summer stationary waves: the opposing effects of direct radiative forcing and sea surface warming *Clim. Dyn.* **53** 4291–309
[46] Luo D, Luo B, Zhang W, Zhuo W, Simmonds I and Yao Y 2024 Arctic amplification-induced intensification of planetary wave modulational instability: a simplified theory of enhanced large-scale waviness *Q. J. R. Meteorol. Soc.* **150** 2888–905
[47] 2019 (available at: https://cds.climate.copernicus.eu)
2024 Version: 3.0.4 (available at: www.metoffice.gov.uk/hadobs/hadex3) (available at: https://esgf-node.llnl.gov/search/cmip6/)
2025 version: 4.09 (available at: https://crudata.uea.ac.uk/cru/data/hrg/cru_ts_4.09/cruts.2503051245.v4.09/tmp/)